AIMS Mathematics, 9(11): 31393–31413.
DOI: 10.3934/math.20241512
Received: 02 September 2024
Revised: 14 October 2024
Accepted: 29 October 2024
Published: 05 November 2024

http://www.aimspress.com/journal/Math

Research article

HIV dynamics in a periodic environment with general transmission rates

Mohammed H. Alharbi*

Department of Mathematics and Statistics, College of Science, University of Jeddah, Jeddah, Saudi Arabia

* **Correspondence:** Email: mhhalharbi1@uj.edu.sa.

Abstract: In the current study, we present a mathematical model for human immunodeficiency virus type-1 (*HIV*-1) transmission, incorporating Cytotoxic T-Lymphocyte immune impairment within a seasonal environment. The model divides the infected cell compartment into two sub-compartments: latently infected cells and productively infected cells. Additionally, we consider three possible routes of infection, allowing *HIV* to spread among susceptible cells via direct contact with the virus, latently infected cells, or productively infected cells. The system is analyzed, and the basic reproduction number is derived using an integral operator. We demonstrate that the *HIV*-free periodic trajectory is globally asymptotically stable if $\mathcal{R}_0 < 1$, while *HIV* persists when $\mathcal{R}_0 > 1$. Several numerical simulations are provided to validate the theoretical results.

Keywords: *HIV* transmission; three infection routes; periodic environment; periodic trajectory; integral operator; uniform persistence
Mathematics Subject Classification: 34K13, 34K20, 34D23

1. Introduction

Human immunodeficiency virus (*HIV*) gradually destroys various types of blood cells, significantly weakening the immune system. Although antiretroviral drugs exist, their effectiveness is often limited, and without treatment, the virus can progress to acquired immunodeficiency syndrome (*AIDS*). *HIV* infections are caused by one of two retroviruses: *HIV*-1 or *HIV*-2. *HIV*-1 is the predominant cause of *HIV* infections globally, while *HIV*-2 is more common in West Africa. Another retrovirus, human T-lymphotropic virus (*HTLV*), although less prevalent, can also cause severe illness. *HIV* primarily targets and gradually depletes $CD4^+$ lymphocytes, a type of white blood cell critical to the body's defense against foreign cells, infections, and cancer. As *HIV* reduces these cells, the immune system becomes increasingly vulnerable to a wide range of opportunistic infections. Consequently, the majority of complications associated with *HIV*, including mortality, result from these secondary

infections rather than the *HIV* infection itself.

Mathematical modeling plays a crucial role in understanding infectious diseases like *HIV* and predicting their long-term behavior. By simulating the evolution of key variables, these models provide valuable insights into the dynamics of the disease. In this context, the model serves as a complementary tool, augmenting our understanding of the complex interactions within the system rather than attempting to replace real-world observations. A significant body of research has focused on the mathematical modeling of *HIV* dynamics, particularly the interaction between *HIV* and T-lymphocytes. These models often employ nonlinear ordinary differential equations to capture the complexity of the system. In [1], Liu and Jiang studied the dynamics of a higher-order stochastically perturbed *HIV/AIDS* model with differential infectivity and amelioration. In [2], Naik et al. studied a dynamical fractional-order *HIV*-1 model by considering the chaotic behavior. In [3], Di Mascio et al. proposed and analyzed a mathematical model for the long-term control of viremia in *HIV*-1 infected patients treated with antiretroviral therapy. In [4], Kumar et al. studied a fractional model of *HIV*-1 infection with the effect of antiviral drug therapy. In [5], Ullah et al. proposed a fractional-order model describing *HIV*-1 transmission under the influence of antiviral drug treatment.

Seasonality is known to have a profound impact on the dynamics of several epidemics, with many displaying periodic behavior. This periodicity can be attributed to factors such as varying contact rates between uninfected and infected individuals, or it may occur autonomously [6–9]. Several studies [10–14] have explored the impact of seasonality on various epidemics, including *HIV* and chikungunya virus transmission. Recently, there has been a growing emphasis on studying *HIV* models from a within-host perspective to obtain a deeper understanding of *HIV* infections, not only in the time-fixed models that gained traction, but also in those considering periodic/seasonal effects. The intricate dynamics of viral infections within host organisms present a compelling area of study, particularly when examining the interplay between various biological and environmental factors that can influence infection outcomes. These factors, which include periodic effects and periodic treatments, can significantly impact the replication of viruses and their interactions with the host, ultimately shaping the course of the infection. While circadian rhythms, the natural cycles of biological processes that occur roughly every 24 hours, serve as a prime example of how timing can regulate physiological functions such as immune responses, other periodic phenomena, such as seasonal variations in contact rates or vaccination programs, can also play a crucial role in disease transmission dynamics. In [15], Wang and Song studied a mathematical model for *HIV* infection with periodic solutions. In [16], the authors examined the influence of periodic variations on *HIV* transmission while in [17], the authors focused on *HIV* infection dynamics with three routes of transmission with linear transmission rates in a periodic environment.

In this study, we refine the modeling of *HIV* dynamics by incorporating three distinct routes of transmission and adopting general nonlinear transmission rates within a seasonal environment, thereby introducing greater realism into the model. The basic reproduction number $\mathcal{R}_0$ is derived using an integral operator. Our analysis reveals that the virus-free periodic trajectory remains globally stable when $\mathcal{R}_0 < 1$, whereas the virus persists periodically when $\mathcal{R}_0 > 1$. These theoretical results are substantiated by comprehensive numerical simulations. The paper is structured as follows: In Section 2, we introduce a system of nonlinear ordinary differential equations that models the dynamics of *HIV* transmission through three distinct routes in a seasonal environment, where the transmission rates are expressed in general nonlinear forms. We demonstrate that the virus-free periodic solution is

globally asymptotically stable when $\mathcal{R}_0 < 1$, and that the virus persists when $\mathcal{R}_0 > 1$. Section 3 provides several numerical examples that support our theoretical findings. Finally, the concluding remarks of our study are presented in Section 4.

2. Mathematical model development

The mathematical model proposed here is a generalization of the one presented in [17], which is a compartmental model describing the transfer between different compartments. We consider the variables S, L, and P to represent the numbers of susceptible, latently infected, and productively infected cells, respectively. Similarly, the variables V and C denote the numbers of free virions (*HIV*-1 particles) and T-lymphocytes, respectively. The infected cells are subdivided into two compartments based on their status: L or P. The variation in the number of infected cells depends on the number of target cells and the incidence rates. The three routes of infection are given by $\sigma_1\varphi_1(V)S$, $\sigma_2\varphi_2(L)S$, and $\sigma_3\varphi_3(P)S$, corresponding to infection from free virions, latently infected cells, and productively infected cells, respectively.

$$\begin{cases} \dot{S}(t) = d_s(t)\Lambda(t) - d_s(t)S(t) - [\sigma_1(t)\varphi_1(V(t)) + \sigma_2(t)\varphi_2(L(t)) + \sigma_3(t)\varphi_3(P(t))]S(t), \\ \dot{L}(t) = [\sigma_1(t)\varphi_1(V(t)) + \sigma_2(t)\varphi_2(L(t)) + \sigma_3(t)\varphi_3(P(t))]S(t) - (\eta_1(t) + d_l(t))L(t), \\ \dot{P}(t) = \eta_1(t)L(t) - d_p(t)P(t) - \sigma_4(t)\varphi_4(P(t))C(t), \\ \dot{V}(t) = \eta_2(t)P(t) - d_v(t)V(t), \\ \dot{C}(t) = \eta_3(t)P(t) - d_c(t)C(t) - \sigma_5(t)\varphi_5(P(t))C(t), \end{cases} \tag{2.1}$$

given an initial condition with non-negative values $(S^0, L^0, P^0, V^0, C^0) \in \mathbb{R}^5_+$. The significance of the model's parameters are given in Table 1.

Note that the incidence rates ($\varphi_1(V)$, $\varphi_2(L)$, and $\varphi_3(P)$), the neutralization rate ($\varphi_4(P)$) and the T-Lymphocyte impairment rate ($\varphi_5(P)$) are all continuous, increasing functions that pass through the origin. Thus, we assume that these functions ($\varphi_1(V)$, $\varphi_2(L)$, $\varphi_3(P)$, $\varphi_4(P)$, and $\varphi_5(P)$) satisfy certain assumptions. Furthermore, we assume that the death rates of the cells are distinct and depend on the cell status.

Assumption 2.1. • *All the model's parameters are ω-periodic nonnegative functions.*

- *φ_1, φ_2, φ_3, φ_4, and φ_5 are continuous increasing functions such that*

$$\varphi_1(0) = \varphi_2(0) = \varphi_3(0) = \varphi_4(0) = \varphi_5(0) = 0.$$

- $d_s(t) \leq d_l(t) \leq d_p(t), \ \forall\ t \in \mathbb{R}_+$.

Let $C(t)$ be a continuous, $n \times n$ matrix function, ω-periodic, irreducible, and cooperative. Let $\xi_C(t)$ be the solution of

$$\dot{\xi}(t) = C(t)\xi(t), \tag{2.2}$$

and $r(\xi_C(\omega))$ the spectral radius of $\xi_C(\omega)$ having positive elements $\forall t > 0$. By applying the famous theory of Perron-Frobenius [18], one can deduce that $\xi_C(\omega)$ has the principal eigenvalue $r(\xi_C(\omega))$. Therefore, we need to use the following lemma several times.

Table 1. Description of variables and parameters.

Note	Significance
S	Susceptible cells
L	Latently infected cells
P	Productively infected cells
V	*HIV*-1 particles
C	T-lymphocytes
$\varphi_1(V)$	Infection rate from V
$\varphi_2(L)$	Infection rate from L
$\varphi_3(P)$	Infection rate from P
$\varphi_4(P)$	Neutralization rate of P
$\varphi_5(P)$	T-lymphocytes impairment rate
η_1	Conversion rate from the L to P
η_3	T-lymphocyte immune rate
σ_1	Periodic contact rate between S and V
σ_2	Periodic contact rate of S and L
σ_3	Periodic contact rate of S and P
σ_4	Periodic neutralization contact rate
σ_5	T-lymphocyte impairment contact rate
d_s	Death rate of S
d_l	Death rate of L
d_p	Death rate of P
d_v	Death rate of V
d_c	Death rate of C
η_2	Generation rate of *HIV* particles
Λ	Generation rate of susceptible cells S

Lemma 2.2 ([19])**.** *The ordinary differential equation (2.2) admits the solution* $\xi(t) = x(t)e^{\ell t}$ *where* $\ell = \dfrac{1}{\omega}\ln(r(\xi_C(\omega)))$ *and the function* $x(t)$ *is positive and* ω*-periodic.*

Consider the one-dimensional equation

$$\dot{S}(t) = d_s(t)(\Lambda(t) - S(t)), \tag{2.3}$$

such that the initial condition $S^0 \in \mathbb{R}_+$. Equation (2.3) has a unique ω-periodic globally attractive solution denoted by $\Lambda^*(t)$ satisfying $\Lambda^*(t) > 0$ for all $t > 0$. As a result, model (2.1) allows for a unique virus-free periodic trajectory denoted $\mathcal{A}_0(t) = (\Lambda^*(t), 0, 0, 0, 0)$.

For any continuous ω-periodic variable $\varphi(t)$, we denote $\varphi^u = \max\limits_{t\in[0,\omega)} \varphi(t)$, $\varphi^l = \min\limits_{t\in[0,\omega)} \varphi(t)$, and $d(t) = \min\limits_{t\geq 0}(d_v(t), d_c(t))$.

Proposition 2.3. $\Omega^u = \left\{(S, L, P, V, C) \in \mathbb{R}^5_+ \ / \ S + L + P \leq \Lambda^u; V + C \leq (\eta_2^u + \eta_3^u)\dfrac{\Lambda^u}{d^l}\right\}$ *is compact,*

positive, invariant, and an attractor of every solution of system (2.1) such that we have

$$\lim_{t\to\infty} S(t) + L(t) + P(t) - \Lambda^*(t) = 0. \tag{2.4}$$

Proof. By summing the first three equations of system (2.1), we obtain

$$\begin{aligned} \dot{S}(t) + \dot{L}(t) + \dot{P}(t) &\leq d_s(t)\Big(\Lambda(t) - (S(t) + L(t) + P(t))\Big) \\ &\leq 0, \text{ if } (S(t) + L(t) + P(t)) \geq \Lambda^u, \end{aligned}$$

and

$$\begin{aligned} \dot{V}(t) + \dot{C}(t) &= (\eta_2(t) + \eta_3(t))P(t) - d_v(t)V(t) - d_c(t)C(t) - \sigma_5(t)\varphi_5(P(t))C(t) \\ &\leq (\eta_2(t) + \eta_3(t))P(t) - d_v(t)V(t) - d_c(t)C(t) \\ &\leq (\eta_2^u + \eta_3^u)\Lambda^u - d(t)(V(t) + C(t)) \\ &\leq 0, \text{ if } d(t)(V(t) + C(t)) \geq (\eta_2^u + \eta_3^u)\Lambda^u. \end{aligned}$$

□

2.1. Disease-free periodic trajectory

By using the theory of Wang and Zhao [20], we can define the basic reproduction number $\mathcal{R}_0$ by rewriting system (2.1) in the following suitable form: Let

$$\begin{aligned} X(t) &= (L(t), P(t), V(t), S(t), C(t))^T, \\ \mathcal{Z}(t, X(t)) &= ((\sigma_1(t)\varphi_1(V(t)) + \sigma_2(t)\varphi_2(L(t)) + \sigma_3(t)\varphi_3(P(t)))S(t), \eta_1(t)L(t), \eta_2(t)P(t), 0, 0)^T, \\ \mathcal{W}^-(t, X(t)) &= ((\eta_1(t) + d_l(t))L(t), d_p(t)P(t) + \sigma_4(t)\varphi_4(P(t))C(t), d_v(t)V(t), \\ &\quad (d_s(t) + \sigma_1(t)\varphi_1(V(t)) + \sigma_2(t)\varphi_2(L(t)) \\ &\quad + \sigma_3(t)\varphi_3(P(t)))S(t), d_c(t)C(t) + \sigma_5(t)\varphi_5(P(t))C(t))^T \end{aligned}$$

and

$$\mathcal{W}^+(t, X(t)) = (0, 0, 0, d_s(t)\Lambda(t), \eta_3(t)P(t))^T.$$

Our goal is to satisfy Assumptions (A1)–(A7) of [20]. Through the new variables' order, (2.1) will be written as

$$\dot{X}(t) = \mathcal{Z}(t, X(t)) - \mathcal{W}(t, X(t)) = \mathcal{Z}(t, X(t)) - \mathcal{W}^-(t, X(t)) + \mathcal{W}^+(t, X(t)). \tag{2.5}$$

Therefore, Assumptions (A1)–(A5) in [20] are already satisfied. (2.5) admits a virus-free periodic trajectory $X^*(t) = (0, 0, 0, \Lambda^*(t), 0)^T$. Let

$$h(t, X(t)) = \mathcal{Z}(t, X(t)) - \mathcal{W}^-(t, X(t)) + \mathcal{W}^+(t, X(t))$$

and

$$M(t) = \left(\frac{\partial \varphi_i(t, X^*(t))}{\partial X_j}\right)_{4\leq i,j\leq 5},$$

where $h_i(t, X(t))$ and $X_i(t)$ are the i-th components of $h(t, X(t))$ and $X(t)$, respectively. We can easily obtain that

$$M(t) = \begin{pmatrix} -d_s(t) & 0 \\ 0 & -d_c(t) \end{pmatrix}.$$

Then, $r(\phi_M(\omega)) < 1$. Then, the disease-free trajectory $X^*(t)$ is asymptotically stable inside Ω_s, where

$$\Omega_s = \left\{(0, 0, 0, S, 0) \in R_+^5\right\},$$

and then Assumption (A6) of [20] is also verified.

Let us define the matrix functions $\mathbf{Z}(t)$ and $\mathbf{W}(t)$ given by

$$\mathbf{Z}(t) = \left(\frac{\partial \mathcal{Z}_i(t, X^*(t))}{\partial X_j}\right)_{1\leq i,j\leq 3}$$

and

$$\mathbf{W}(t) = \left(\frac{\partial \mathcal{W}_i(t, X^*(t))}{\partial X_j}\right)_{1\leq i,j\leq 3}$$

such that $\mathcal{Z}_i(t, X(t))$ and $\mathcal{W}_i(t, X(t))$ are the i-th components of $\mathcal{Z}(t, X(t))$ and $\mathcal{W}(t, X(t))$, respectively. By a simple calculation, we obtain

$$\mathbf{Z}(t) = \begin{pmatrix} \sigma_2(t)\varphi_2'(0)\Lambda^*(t) & \sigma_3(t)\varphi_3'(0)\Lambda^*(t) & \sigma_1(t)\varphi_1'(0)\Lambda^*(t) \\ \eta_1(t) & 0 & 0 \\ 0 & \eta_2(t) & 0 \end{pmatrix}$$

and

$$\mathbf{W}(t) = \begin{pmatrix} \eta_1(t) + d_l(t) & 0 & 0 \\ 0 & d_p(t) & 0 \\ 0 & 0 & d_v(t) \end{pmatrix}.$$

The expression $\frac{d}{dt}H(t_1, t_2) = -\mathbf{W}(t_1)H(t_1, t_2)$ with $t_1 \geq t_2$ and $H(t_1, t_1) = I_3$ admits a 3×3 matrix solution denoted by $H(t_1, t_2)$. Then, Assumption (A7) of [20] is also verified.

Let us define the linear operator $K : C_\omega \to C_\omega$ as

$$(K\phi)(p) = \int_0^\infty H(p, p - s)\mathbf{Z}(p - s)\phi(p - s)ds, \ \forall p \in \mathbb{R}, \phi \in C_\omega \tag{2.6}$$

where C_ω is the Banach space of ω-periodic functions $\mathbb{R} \mapsto \mathbb{R}^3$, equipped with $\|.\|_\infty$ as its norm. Therefore, the basic reproduction number $\mathcal{R}_0$ is expressed as the spectral radius of the operator K:

$$\mathcal{R}_0 = r(K).$$

Furthermore, according to the theory in [20, Theorem 2.2], we have the following results.

Theorem 2.4. *[20, Theorem 2.2]*

- $\mathcal{R}_0 < 1 \ \Leftrightarrow \ r(\phi_{Z-W}(\omega)) < 1.$
- $\mathcal{R}_0 = 1 \ \Leftrightarrow \ r(\phi_{Z-W}(\omega)) = 1.$
- $\mathcal{R}_0 > 1 \ \Leftrightarrow \ r(\phi_{Z-W}(\omega)) > 1.$

Thus, the local asymptotic stability of $\mathcal{A}_0(t)$ is conditional to the satisfaction of the condition where $\mathcal{R}_0 < 1$; else, it will be unstable if $\mathcal{R}_0 > 1$.

Theorem 2.5. *The global asymptotic stability of the disease-free solution, $\mathcal{A}_0(t)$, is conditional to the satisfaction of the condition where $\mathcal{R}_0 < 1$, and it will be unstable if $\mathcal{R}_0 > 1$.*

Proof. According to Theorem 2.4, the local asymptotic stability of $\mathcal{A}_0(t)$ is conditional to $\mathcal{R}_0 < 1$. Therefore, we have to show that $\mathcal{A}_0(t)$ is a globally attractive solution for the case where $\mathcal{R}_0 < 1$. By reference to the limit (2.4) in Lemma 2.3, $\forall\ \varsigma_1 > 0$, $\exists\, T_1 > 0$ satisfying $S(t) + L(t) + P(t) \leq \Lambda^*(t) + \varsigma_1$, $\forall\, t > T_1$. Then, $S(t) \leq \Lambda^*(t) + \varsigma_1$, and

$$\begin{cases} \dot{L}(t) \leq [\sigma_1(t)\varphi_1(V(t)) + \sigma_2(t)\varphi_2(L(t)) + \sigma_3(t)\varphi_3(P(t))](\Lambda^*(t) + \varsigma_1) - (\eta_1(t) + d_l(t))L(t), \\ \dot{P}(t) = \eta_1(t)L(t) - d_p(t)P(t) - \sigma_4(t)\varphi_4(P(t))C(t), \\ \dot{V}(t) = \eta_2(t)P(t) - d_v(t)V(t), \end{cases} \tag{2.7}$$

$\forall\, t > T_1$. Let us consider the matrix

$$M_2(t) = \begin{pmatrix} \sigma_2(t)\varphi_2'(0) & \sigma_3(t)\varphi_3'(0) & \sigma_1(t)\varphi_1'(0) \\ 0 & 0 & 0 \\ 0 & 0 & 0 \end{pmatrix}. \tag{2.8}$$

By using Theorem 2.4, we have $r(\varphi_{Z-W}(\omega)) < 1$, and then we can choose $\varsigma_1 > 0$ small enough to satisfy $r(\varphi_{Z-W+\varsigma_1 M_2}(\omega)) < 1$, and we consider the following system:

$$\begin{cases} \dot{\bar{Y}}_l(t) = [\sigma_1(t)\varphi_1(\bar{V}(t)) + \sigma_2(t)\varphi_2(\bar{L}(t)) + \sigma_3(t)\varphi_3(\bar{P}(t))](\Lambda^*(t) + \varsigma_1) - (\eta_1(t) + d_l(t))\bar{L}(t), \\ \dot{\bar{Y}}_i(t) = \eta_1(t)L(t) - d_p(t)\bar{P}(t) - \sigma_4(t)\varphi_4(\bar{P}(t))\bar{C}(t), \\ \dot{\bar{Y}}_v(t) = \eta_2(t)\bar{P}(t) - d_v(t)\bar{V}(t). \end{cases} \tag{2.9}$$

According to Lemma 2.2 and the comparison principle, we can prove that $\exists\, y(t)$, an ω-periodic positive function $y_1(t)$ that satisfies $x(t) \leq y(t)e^{k_1 t}$, where

$$x(t) = (L(t), P(t), V(t))$$

and

$$k_1 = \frac{1}{\omega}\ln\left(r(\varphi_{Z-W+\varsigma_1 M_2}(\omega)\right) < 0.$$

Hence, $\lim_{t\to\infty} L(t) = \lim_{t\to\infty} P(t) = \lim_{t\to\infty} V(t) = 0$, and then $\lim_{t\to\infty} C(t) = 0$. Furthermore, according to Eq (2.4), we deduce that $\lim_{t\to\infty}(S(t) - \Lambda^*(t)) = 0$. We conclude the global attractivity of $\mathcal{A}_0(t)$, enabling us to finalize the proof. □

2.2. HIV-infected periodic trajectory

Consider the Poincaré map $Q : \mathbb{R}^5_+ \to \mathbb{R}^5_+$ applied to system (2.1) where $Y_0 \mapsto w(\omega, Y^0)$ and $w(t, Y^0)$ is a trajectory of system (2.1) such that $w(0, Y^0) = Y^0 \in \mathbb{R}^4_+$ is the initial condition. Let us define the sets $\Gamma = \left\{(S, L, P, V, C) \in \mathbb{R}^5_+\right\}$, $\Gamma_0 = Int(\mathbb{R}^5_+)$, and $\partial\Gamma_0 = \Gamma \setminus \Gamma_0$. By using Lemma 2.3, it is easy to see that Γ and Γ_0 are positively invariant and that Q is point dissipative. Let us consider

$$M_\partial = \left\{(S^0, L^0, P^0, V^0, C^0) \in \partial\Gamma_0 : Q^n(S^0, L^0, P^0, V^0, C^0) \in \partial\Gamma_0,\ \forall\, n \geq 0\right\}.$$

Before applying the uniform persistence theory [19, 21], we have to demonstrate that

$$M_\partial = \{(S, 0, 0, 0, 0),\ S \geq 0\}. \tag{2.10}$$

On the one hand, we have $M_\partial \supseteq \{(S,0,0,0,0),\ S \geq 0\}$, and it remains to be shown that $M_\partial \setminus \{(S,0,0,0,0),\ S \geq 0\} = \emptyset$. Let

$$(S^0, L^0, P^0, V^0, C^0) \in M_\partial \setminus \{(S,0,0,0,0),\ S \geq 0\}.$$

Once $P^0 = 0$ and $0 < L^0$, $L(t) > 0$, $\forall\, t > 0$. Therefore, we obtain $\dot{P}(t)_{|t=0} = \eta_1(0)L^0 > 0$. Once $P^0 > 0$ and $L^0 = 0$, $P(t) > 0$ and $S(t) > 0$, $\forall\, t > 0$. Then, $\forall\, t > 0$, one has

$$\begin{aligned} L(t) &= \Big[L^0 + \int_0^t [\sigma_1(\theta)\varphi_1(V(\theta)) + \sigma_2(\theta)\varphi_2(L(\theta)) \\ &\quad + \sigma_3(\theta)\varphi_3(P(\theta))]S(\theta)e^{\int_0^\theta (\eta_1(s)+d_l(s))ds}\, d\theta\Big] e^{-\int_0^t (\eta_1(s)+d_l(s))ds} > 0 \end{aligned}$$

$\forall\, t > 0$, which means that $(S(t), L(t), P(t), V(t), C(t)) \notin \partial\Gamma_0$ for $0 < t$. Eq (2.10) follows directly since Γ_0 is positively invariant, as established in Proposition 2.3. Subsequently, $\exists\, (\Lambda^*(0), 0, 0, 0, 0)$, a unique fixed point of Q in M_∂, and the *HIV* will persist.

Theorem 2.6. *If $\mathcal{R}_0 > 1$, then* (2.1) *admits at least a positive periodic solution. Furthermore, $\exists\, \varrho > 0$ that satisfies $\forall\ (S^0, L^0, P^0, V^0, C^0) \in \mathbb{R}_+ \times Int(\mathbb{R}^5_+)$,*

$$\liminf_{t\to\infty} P(t) \geq \varrho > 0.$$

Proof. We aim in this proof to use the theory in reference [21, Theorem 3.1.1] to demonstrate the uniform persistence of the Poincaré map Q respecting $(\Gamma_0, \partial\Gamma_0)$, which allows us to prove the uniform persistence of the trajectories of system (2.1) respecting $(\Gamma_0, \partial\Gamma_0)$. Note that $r(\varphi_{Z-W}(\omega)) > 1$ according to Theorem 2.4. Then, we can choose a constant $\varsigma_2 > 0$ such that $r(\varphi_{Z-W-\varsigma_2 M_2}(\omega)) > 1$. Consider the perturbed dynamics

$$\dot{S}_\alpha(t) = d_s(t)\Lambda(t) - d_s(t)S_\alpha(t) - [\sigma_1(t)\varphi_1(\alpha) + \sigma_2(t)\varphi_2(\alpha) + \sigma_3(t)\varphi_3(\alpha)]S_\alpha(t). \tag{2.11}$$

The Poincaré map Q admits a unique fixed point $\bar{S}^0_\alpha$ that is continuous with respect to α. Thus, one can choose $\alpha > 0$ satisfying $\bar{S}_\alpha(t) > \bar{S}(t) - \varsigma_2,\ \ \forall\ t > 0$. Let us denote $M_1 = (\bar{S}^0, 0, 0, 0, 0)$. Since each solution of the dynamics is continuous with respect to the initial condition, then $\exists\, \alpha^*$ satisfies $\forall\ (S^0, L^0, P^0, V^0, C^0) \in \Gamma_0$ with $\|(S^0, L^0, P^0, V^0, C^0) - M_1\| \leq \alpha^*$, and we obtain that

$$\|w(t, (S^0, L^0, P^0, V^0, C^0)) - w(t, M_1)\| < \alpha \text{ for } 0 \leq t \leq \omega.$$

By using the contradiction process, we will demonstrate that

$$\limsup_{n\to\infty}\ d(Q^n(S^0, L^0, P^0, V^0, C^0), M_1) \geq \alpha^* \text{ for any } (S^0, L^0, P^0, V^0, C^0) \in \Gamma_0. \tag{2.12}$$

Assume that $\limsup_{n\to\infty} d(Q^n(S^0, L^0, P^0, V^0, C^0), M_1) < \alpha^*$ for some $(S^0, L^0, P^0, V^0, C^0) \in \Gamma_0$. In particular, assume that $d(Q^n(S^0, L^0, P^0, V^0, C^0), M_1) < \alpha^*$, $\forall n > 0$. Therefore, we get

$$\|w(t, Q^n(S^0, L^0, P^0, V^0, C^0)) - w(t, M_1)\| < \alpha$$

for all $n > 0$ and $0 \leq t \leq \omega$. For any $t \geq 0$, assume that $t = n\omega + t_1$, where $t_1 \in [0, \omega)$ and $n \leq \frac{t}{\omega}$ is the greatest integer of $\frac{t}{\omega}$. Then, we get

$$\|w(t, (S^0, L^0, P^0, V^0, C^0)) - w(t, M_1)\| = \|w(t_1, Q^n(S^0, L^0, P^0, V^0, C^0)) - w(t_1, M_1)\| < \alpha, \ \forall\ t \geq 0.$$

Let

$$(S(t), L(t), P(t), V(t), C(t)) = w(t, (S^0, L^0, P^0, V^0, C^0)).$$

Then, $0 \leq L(t), P(t), V(t) \leq \alpha$, $\forall\ t \geq 0$, and

$$\dot{S}(t) \ \geq \ d_s(t)\Lambda(t) - d_s(t)S(t) - (\sigma_1(t)\varphi_1(\alpha) + \sigma_2(t)\varphi_2(\alpha) + \sigma_3(t)\varphi_3(\alpha))S(t). \tag{2.13}$$

The Poincaré map Q has a fixed point $\bar{S}^0_\alpha$ which is globally attractive such that $\bar{S}_\alpha(t) > \bar{S}(t) - \varsigma_2$. Then, there exists a constant $T_2 > 0$ satisfying

$$\bar{S}(t) > \bar{S}(t) - \varsigma_2, \ \forall\ t > T_2.$$

Therefore, $\forall\ t > T_2$,

$$\begin{cases} \dot{L}(t) & \geq & [\sigma_1(t)\varphi_1(V(t)) + \sigma_2(t)\varphi_2(L(t)) + \sigma_3(t)\varphi_3(P(t))](\bar{S}(t) - \zeta) - (\eta_1(t) + d_l(t))L(t), \\ \dot{P}(t) & = & \eta_1(t)L(t) - d_p(t)P(t) - \sigma_4(t)\varphi_4(P(t))C(t), \\ \dot{V}(t) & = & \eta_2(t)P(t) - d_v(t)V(t). \end{cases} \tag{2.14}$$

As $r(\varphi_{Z-W-\varsigma_2 M_2}(\omega)) > 1$, there exists an ω-periodic solution $y(t)$ that satisfies $J(t) \geq e^{k_2 t}y(t)$ and

$$k_2 = \frac{1}{\omega} \ln\ r\left(\varphi_{Z-W-\varsigma_2 M_2}(\omega)\right) > 0.$$

Then, $\lim\limits_{t\to\infty} P(t) = \infty$, and this is impossible since the trajectory is bounded, and so (2.12) is satisfied. The weak uniform persistence of Q is verified with respect to $(\Gamma_0, \partial\Gamma_0)$. According to Proposition 2.3, the map Q admits a global attractor, and then $M_1 = (\bar{S}^0, 0, 0, 0, 0)$ is invariant in Γ and $W^s(M_1) \cap \Gamma_0 = \emptyset$. All solutions inside M_∂ tend towards M_1, which is acyclic in M_∂. By using the results in [21, Theorem 1.3.1], we deduce that the map Q is uniformly persistent with respect to $(\Gamma_0, \partial\Gamma_0)$. Furthermore, when using [21, Theorem 1.3.6], the map Q has a fixed point $(\tilde{S}^0, \tilde{L}^0, \tilde{P}^0, \tilde{V}^0, \tilde{C}^0) \in \Gamma_0$ such that $(\tilde{S}^0, \tilde{L}^0, \tilde{P}^0, \tilde{V}^0, \tilde{C}^0) \in R_+ \times Int(R^4_+)$. Our goal now is to demonstrate that $\tilde{S}^0 > 0$. We shall use the contradiction technique by assuming that $\tilde{S}^0 = 0$. According to system (2.1), $\tilde{S}(t)$ fulfills

$$\dot{\tilde{S}}(t) \geq d_s(t)\Lambda(t) - d_s(t)\tilde{S}(t) - (\sigma_1(t)\varphi_1(\tilde{V}(t)) + \sigma_2(t)\varphi_2(\tilde{L}(t)) + \sigma_3(t)\varphi_3(\tilde{P}(t)))\tilde{S}(t), \tag{2.15}$$

with $\tilde{S}^0 = \tilde{S}(m\omega) = 0, m = 1, 2, 3, \cdots$. By using Lemma 2.3, $\forall\ \varsigma_3 > 0$, $\exists\, T_3 > 0$ satisfying

$$\tilde{L}(t), \tilde{P}(t), \tilde{V}(t) \leq \bar{N} + \varsigma_3, t > T_3.$$

Then, one gets

$$\dot{\tilde{S}}(t) \geq d_s(t)\Lambda(t) - d_s(t)\tilde{S}(t) - (\sigma_1(t)\varphi_1((\bar{N} + \varsigma_3)) + \sigma_2(t)\varphi_2((\bar{N} + \varsigma_3)) + \sigma_3(t)\varphi_3((\bar{N} + \varsigma_3)))\tilde{S}(t)$$

for $t \geq T_3$. Therefore, $\exists\, \bar{m}$ satisfying $m\omega > T_3$, $\forall\, m > \bar{m}$. According to the comparison principle, one obtains

$$\begin{aligned}\tilde{S}(m\omega) &= e^{-\int_0^{m\omega}([\sigma_1(u)\varphi_1(\bar{N}+\varsigma_3)+\sigma_2(u)\varphi_2(\bar{N}+\varsigma_3)+\sigma_3(u)\varphi_3(\bar{N}+\varsigma_3)]+d_s(u))du} \\ &\quad \Big[\tilde{S}^0 + \int_0^{m\omega} d_s(\theta)\Lambda(\theta)e^{\int_0^{\theta}\left([\sigma_1(u)\varphi_1(\bar{N}+\varsigma_3)+\sigma_2(u)\varphi_2(\bar{N}+\varsigma_3)+\sigma_3(u)\varphi_3(\bar{N}+\varsigma_3)]+d_s(u)\right)du} d\theta\Big].\end{aligned}$$

$\tilde{S}(m\omega) > 0$, $\forall\, m > \bar{m}$ which contradicts the fact that $\tilde{S}(m\omega) = 0$. Therefore, $\tilde{S}^0$ should satisfy $\tilde{S}^0 > 0$, and $(\tilde{S}^0, \tilde{L}^0, \tilde{P}^0, \tilde{V}^0, \tilde{C}^0)$ is an ω-periodic solution of (2.1). □

3. Numerical investigation

The goal of this section is to give several numerical tests that confirm the obtained theoretical results. The incidence rates were modeled by Monod-type functions as follows:

$$\varphi_i(X) = \frac{\varphi_i^{max} X}{k_i + X},$$

where φ_i^{max} and k_i, $i = 1, \cdots, 5$ are nonnegative constants. Note that φ_i, $i = 1, \cdots, 5$ are continuous and increasing functions. The ω-periodic functions were modeled by a well-known form given by

$$a(t) = a_0(1 + a_1 \cos(2p\pi(t + \Theta))),$$

where $a_0 \geq 0$ is the baseline value, $0 < a_1 \leq 1$ is the magnitude of the periodic variation, and $0 \leq \Theta \leq 1$ is the phase.

$$\begin{cases} \Lambda(t) = \Lambda_0(1 + \Lambda_1 \cos(2p\pi(t+\Theta))), & d_s(t) = d_{s0}(1 + d_{s1} \cos(2p\pi(t+\Theta))), \\ \sigma_1(t) = \sigma_{10}(1 + \sigma_{11} \cos(2p\pi(t+\Theta))), & d_l(t) = d_{l0}(1 + d_{l1} \cos(2p\pi(t+\Theta))), \\ \sigma_2(t) = \sigma_{20}(1 + \sigma_{21} \cos(2p\pi(t+\Theta))), & d_p(t) = d_{i0}(1 + d_{i1} \cos(2p\pi(t+\Theta))), \\ \sigma_3(t) = \sigma_{30}(1 + \sigma_{31} \cos(2p\pi(t+\Theta))), & d_v(t) = d_{v0}(1 + d_{v1} \cos(2p\pi(t+\Theta))), \\ \sigma_4(t) = \sigma_{40}(1 + \sigma_{41} \cos(2p\pi(t+\Theta))), & d_c(t) = d_{c0}(1 + d_{c1} \cos(2p\pi(t+\Theta))), \\ \sigma_5(t) = \sigma_{50}(1 + \sigma_{51} \cos(2p\pi(t+\Theta))), & \eta_2(t) = \eta_{20}(1 + \eta_{21} \cos(2p\pi(t+\Theta))), \\ \eta_1(t) = \eta_{10}(1 + \eta_{11} \cos(2p\pi(t+\Theta))), & \eta_3(t) = \eta_{30}(1 + \eta_{31} \cos(2p\pi(t+\Theta))). \end{cases} \tag{3.1}$$

The seasonal cycles frequencies Λ_1, d_{s1}, d_{l1}, d_{i1}, d_{v1}, d_{c1}, σ_{11}, σ_{21}, σ_{31}, σ_{41}, σ_{51}, η_{11}, η_{21}, and η_{31} satisfy $|\Lambda_1| < 1$, $|d_{s1}| < 1$, $|d_{l1}| < 1$, $|d_{i1}| < 1$, $|d_{v1}| < 1$, $|d_{c1}| < 1$, $|\sigma_{11}| < 1$, $|\sigma_{21}| < 1$, $|\sigma_{31}| < 1$, $|\sigma_{41}| < 1$, $|\sigma_{51}| < 1$, $|\eta_{11}| < 1$, $|\eta_{21}| < 1$, and $|\eta_{31}| < 1$. All fixed constants Λ_0, m_{s0}, d_{l0}, d_{p0}, d_{v0}, d_{c0}, σ_{10}, σ_{20}, σ_{30}, η_{10}, σ_{40}, σ_{50}, η_{20}, and η_{30} are provided in Table 2. Due to the absence of biological data for our simulations, we have selected parameter values arbitrarily, and they do not possess any biological meaning.

Table 2. Parameters' numerical values.

Λ_0	d_{s0}	d_{l0}	d_{p0}	d_{v0}	d_{c0}
10	0.8	0.7	2	0.5	1
Λ_1	d_{s1}	d_{l1}	d_{p1}	d_{v1}	d_{c1}
10	0.8	0.7	2	0.5	1
φ_4^{max}	φ_5^{max}	k_4	k_5	Θ	p
10	0.8	0.7	2	4	1
σ_{10}	σ_{20}	σ_{30}	η_{10}		
0.2	0.8	4	2		
σ_{40}	σ_{50}	η_{20}	η_{30}		
0.5	1	0.2	0.8		
σ_{11}	σ_{21}	σ_{31}	σ_{41}		
0.2	0.8	4	2		
σ_{51}	η_{11}	η_{21}	η_{31}		
0.5	1	0.2	0.8		

Three environmental situations were considered. The first case involves all parameters being constants. The second case considers only the transmission rates $\sigma_1(t)$, $\sigma_2(t)$, $\sigma_3(t)$, $\sigma_4(t)$, and $\sigma_5(t)$ as ω-periodic functions. The third situation examines the scenario where all parameters are ω-periodic functions.

3.1. Fixed parameters

In this first situation, we consider the case where all parameters are constant. Model (2.1) then takes the form

$$\begin{cases} \dot{S}(t) = d_{s0}\Lambda_0 - d_{s0}S(t) - [\sigma_{10}\varphi_1(V(t)) + \sigma_{20}\varphi_2(L(t)) + \sigma_{30}\varphi_3(P(t))]S(t), \\ \dot{L}(t) = [\sigma_{10}\varphi_1(V(t)) + \sigma_{20}\varphi_2(L(t)) + \sigma_{30}\varphi_3(P(t))]S(t) - (\eta_{10} + d_{l0})L(t), \\ \dot{P}(t) = \eta_{10}L(t) - d_{i0}(t)P(t) - \sigma_{40}\varphi_4(P(t))C(t), \\ \dot{V}(t) = \eta_{20}P(t) - d_{v0}V(t), \\ \dot{C}(t) = \eta_{30}P(t) - d_{c0}C(t) - \sigma_{50}\varphi_5(P(t))C(t), \end{cases} \tag{3.2}$$

such that the positive initial condition $(S^0, L^0, P^0, V^0, C^0) = (0.01, 4, 7, 3, 6) \in \mathbb{R}^5_+$. Let us denote by $\mathcal{R}_0$, the basic reproduction number. It can be determined through the next-generation matrix method [22, 23]. Let

$$F = \begin{pmatrix} \sigma_{20}\varphi_2'(0)\Lambda_0 & \sigma_{30}\varphi_3'(0)\Lambda_0 & \sigma_{10}\varphi_1'(0)\Lambda_0 \\ 0 & 0 & 0 \\ 0 & 0 & 0 \end{pmatrix},$$

$$V = \begin{pmatrix} \eta_{10} + d_{l0} & 0 & 0 \\ -\eta_{10} & d_{p0} & 0 \\ 0 & -\eta_{20} & d_{v0} \end{pmatrix},$$

and then

$$V^{-1} = \begin{pmatrix} \dfrac{1}{\eta_{10}+d_{l0}} & 0 & 0 \\ \dfrac{\eta_{10}}{d_{p0}(\eta_{10}+d_{l0})} & \dfrac{1}{d_{p0}} & 0 \\ \dfrac{\eta_{10}\eta_{20}}{d_{p0}d_{v0}(\eta_{10}+d_{l0})} & \dfrac{\eta_{20}}{d_{i0}d_{v0}} & \dfrac{1}{d_{v0}} \end{pmatrix}.$$

Therefore, the next-generation matrix FV^{-1} is given by

$$\Lambda_0 \begin{pmatrix} \dfrac{\eta_{10}\eta_{20}\sigma_{10}\varphi_1'(0)+d_{p0}d_{v0}\sigma_{20}\varphi_2'(0)+\eta_{10}d_{v0}\sigma_{30}\varphi_3'(0)}{d_{p0}d_{v0}(\eta_{10}+d_{l0})} & \dfrac{\eta_{20}\sigma_{10}\varphi_1'(0)+d_{v0}\sigma_{30}\varphi_3'(0)}{d_{p0}d_{v0}} & \dfrac{\sigma_{10}\varphi_1'(0)}{d_{v0}} \\ 0 & 0 & 0 \\ 0 & 0 & 0 \end{pmatrix}.$$

Therefore, $\mathcal{R}_0$ is given by

$$\mathcal{R}_0 = \Lambda_0 \frac{\eta_{10}\eta_{20}\sigma_{10}\varphi_1'(0)+d_{p0}d_{v0}\sigma_{20}\varphi_2'(0)+\eta_{10}d_{v0}\sigma_{30}\varphi_3'(0)}{d_{p0}d_{v0}(\eta_{10}+d_{l0})}.$$

We provide several numerical examples to validate the obtained theoretical results. The behavior of the trajectories of (3.2) with respect to time is shown in Figure 1 (right) and in *LPV* coordinates in Figure 1 (left), which represent the main variables of the disease where $\mathcal{R}_0 > 1$. As can be seen, the solution converges to the positive steady state, reflecting the persistence of *HIV*. To validate global stability, we consider several initial conditions in Figure 2, and all trajectories converge to the same steady state. In Figure 3 (left), the behavior of the trajectories of (3.2) in *LPV* coordinates and the behavior of the trajectories with respect to time (Figure 3, right) are shown for $\mathcal{R}_0 < 1$. Once again, the theoretical results are confirmed, as the solution converges to the *HIV* disease-free steady state $\mathcal{A}_0 = (\Lambda_0, 0, 0, 0, 0)$, confirming the extinction of *HIV*. To further validate the global stability of the *HIV* disease-free steady state $\mathcal{A}_0$, several initial conditions were considered in Figure 4, and all trajectories converge to the same disease-free steady state.

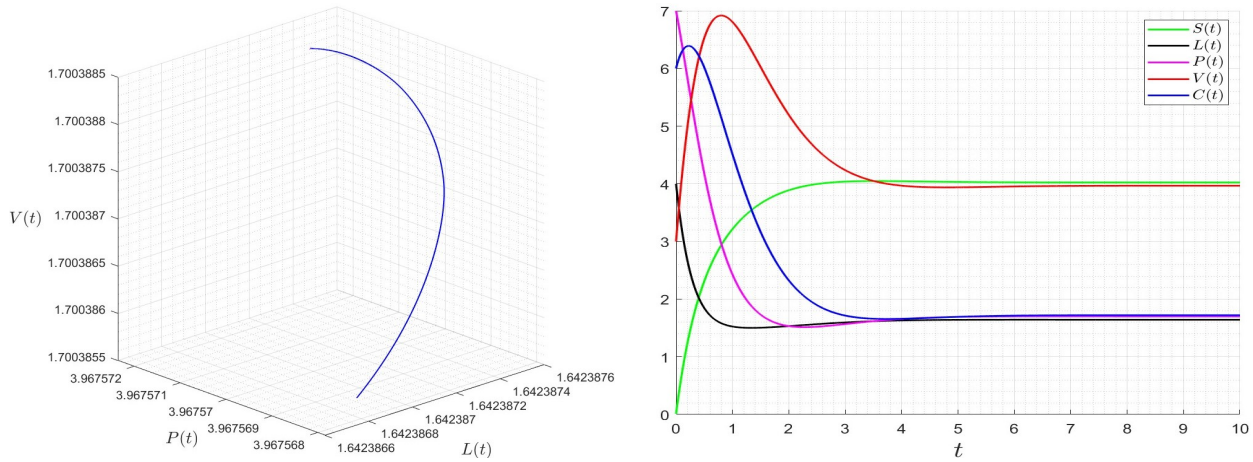

Figure 1. Dynamics of (3.2) for $\varphi_1^{max} = 0.2$, $\varphi_2^{max} = 0.3$, $\varphi_3^{max} = 0.4$, $k_1 = 1$, $k_2 = 2$, and $k_3 = 3$, whit $\mathcal{R}_0 \approx 7.15 > 1$.

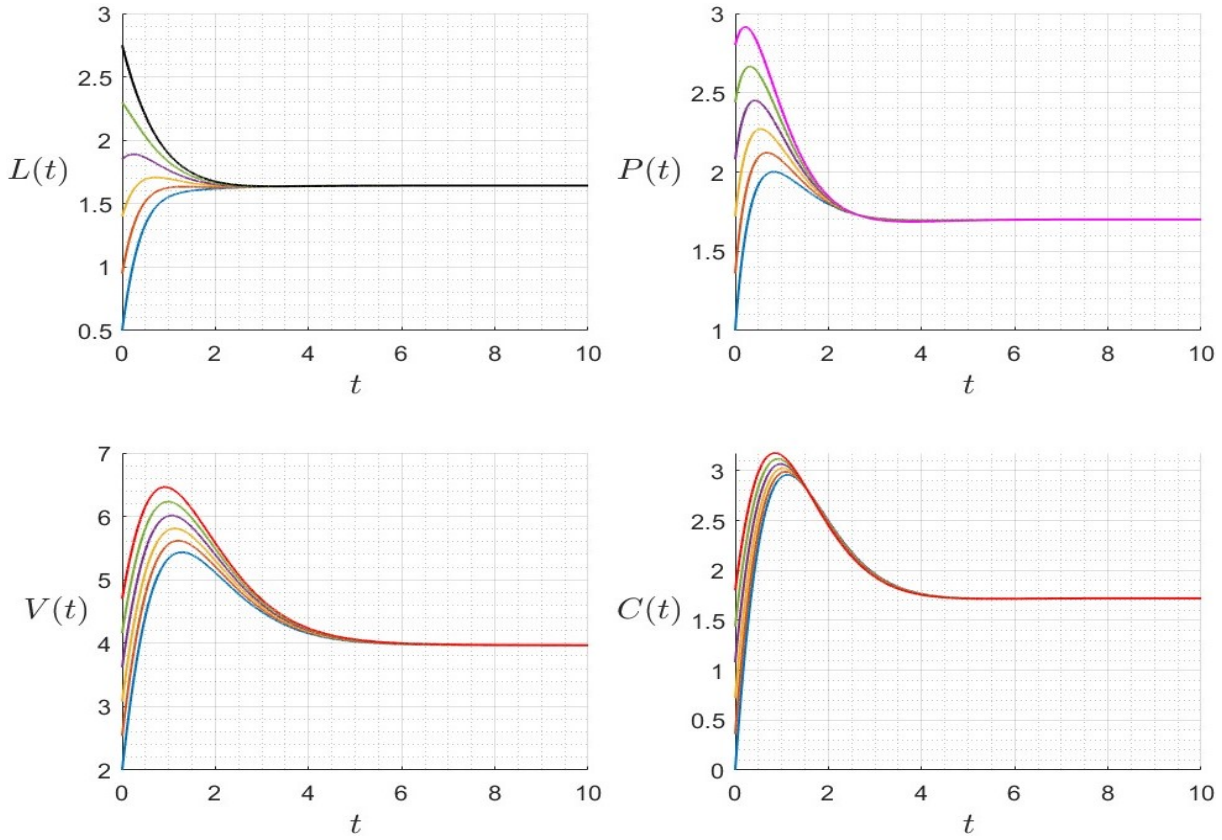

Figure 2. Behavior of the trajectories of (3.2) for several initial conditions when $\varphi_1^{max} = 0.2$, $\varphi_2^{max} = 0.3$, $\varphi_3^{max} = 0.4$, $k_1 = 1$, $k_2 = 2$, and $k_3 = 3$, with $\mathcal{R}_0 \approx 7.15 > 1$.).

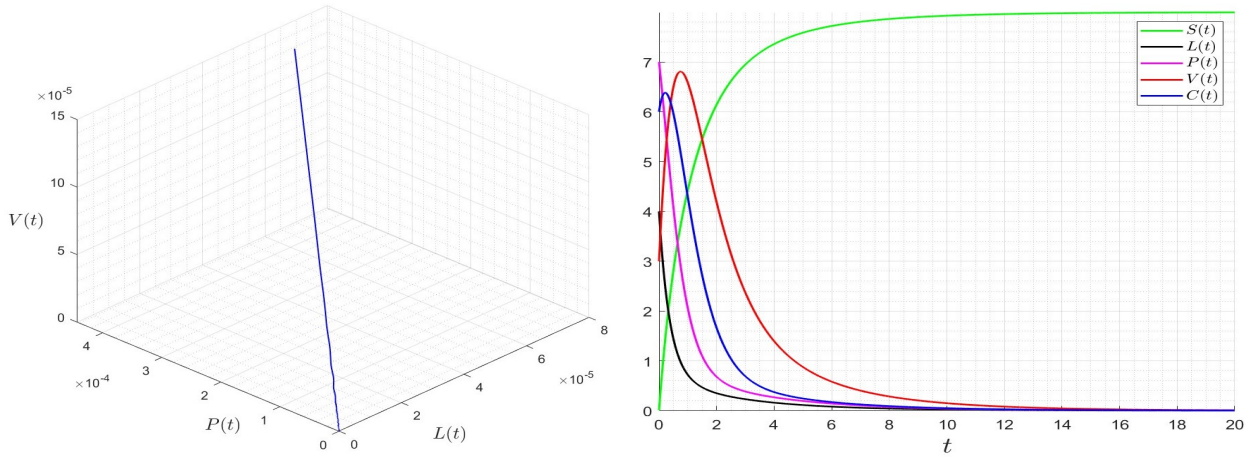

Figure 3. Dynamics of (3.2) for $\varphi_1^{max} = 0.1$, $\varphi_2^{max} = 0.2$, $\varphi_3^{max} = 0.3$, $k_1 = 12$, $k_2 = 12$, and $k_3 = 12$, with $\mathcal{R}_0 \approx 0.58 < 1$.

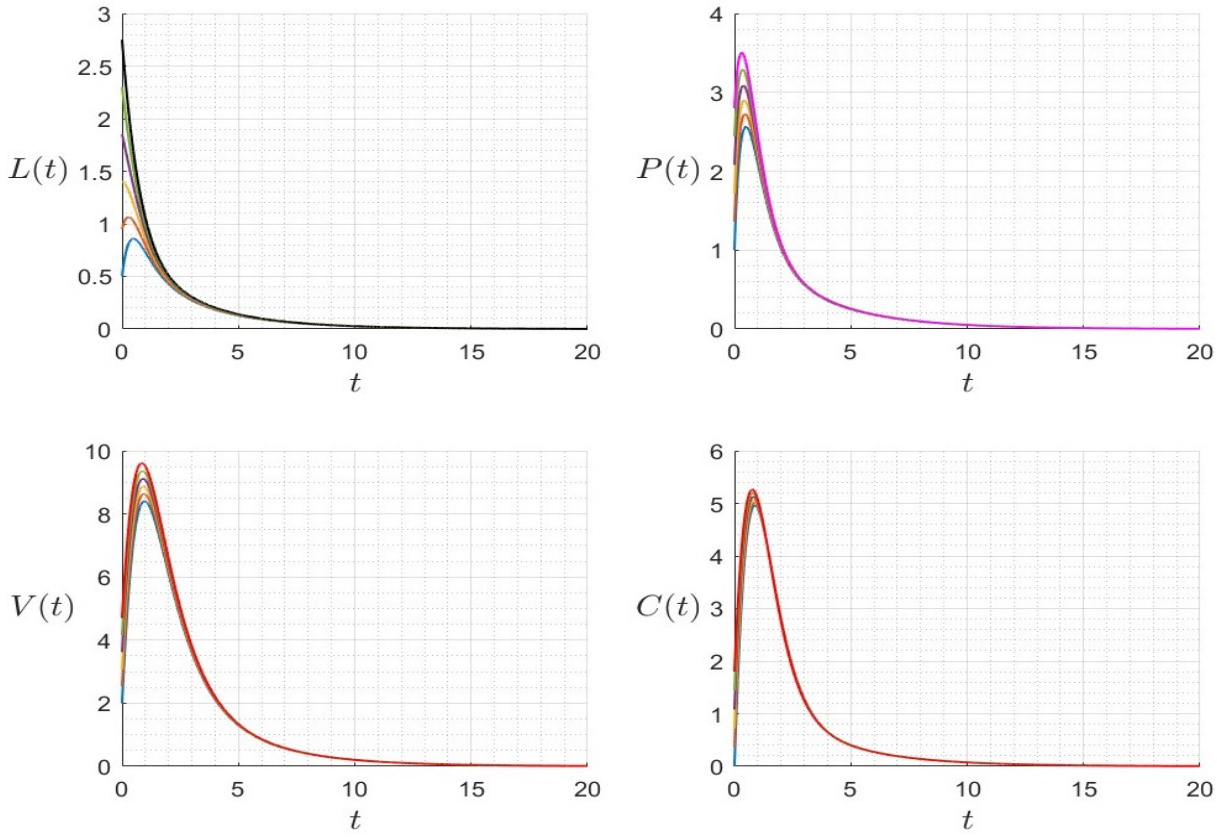

Figure 4. Behavior of the trajectories of (3.2) for several initial conditions when $\varphi_1^{max} = 0.1$, $\varphi_2^{max} = 0.2$, $\varphi_3^{max} = 0.3$, $k_1 = 12$, $k_2 = 12$, and $k_3 = 12$ ($\mathcal{R}_0 \approx 0.58 < 1$).

3.2. Periodic transmission rates

In the second situation, we perform numerical tests on (2.1), where only the incidence rates ($\sigma_1(t)$, $\sigma_2(t)$, $\sigma_3(t)$), the neutralization rate ($\sigma_4(t)$), and the T-lymphocytes impairment rate ($\sigma_5(t)$) depend on time t, and are assumed to be ω-periodic functions. The model then takes the form

$$\begin{cases} \dot{S}(t) = d_{s0}\Lambda_0 - d_{s0}S(t) - [\sigma_1(t)\varphi_1(V(t)) + \sigma_2(t)\varphi_2(L(t)) + \sigma_3(t)\varphi_3(P(t))]S(t), \\ \dot{L}(t) = [\sigma_1(t)\varphi_1(V(t)) + \sigma_2(t)\varphi_2(L(t)) + \sigma_3(t)\varphi_3(P(t))]S(t) - (\eta_{10} + d_{l0})L(t), \\ \dot{P}(t) = \eta_{10}L(t) - d_{i0}(t)P(t) - \sigma_4(t)\varphi_4(P(t))C(t), \\ \dot{V}(t) = \eta_{20}P(t) - d_{v0}V(t), \\ \dot{C}(t) = \eta_{30}P(t) - d_{c0}C(t) - \sigma_5(t)\varphi_5(P(t))C(t), \end{cases} \tag{3.3}$$

such that the positive initial condition $(S^0, L^0, P^0, V^0, C^0) = (0.01, 4, 7, 3, 6) \in \mathbb{R}^5_+$. We used the time-averaged system to approximate $\mathcal{R}_0$. The behavior of the trajectories of (3.3) with respect to time is shown in Figure 5 (right), and in *LPV* coordinates in Figure 5 (left), where $\mathcal{R}_0 > 1$. As can be seen, the solution converges to a periodic trajectory, confirming *HIV* persistence. Several initial conditions were considered in Figure 6, and all trajectories converge to the same periodic solution. In Figure 7, we display the behavior of the trajectories of (3.3) in *LPV* coordinates (left) and with respect to time

(right) for $\mathcal{R}_0 < 1$. Again, the theoretical results are confirmed, as the solution converges to the *HIV* disease-free steady state $\mathcal{A}_0 = (\Lambda_0, 0, 0, 0, 0)$, confirming *HIV* extinction. In Figure 8, several initial conditions were considered, and all trajectories converge to the same disease-free steady state.

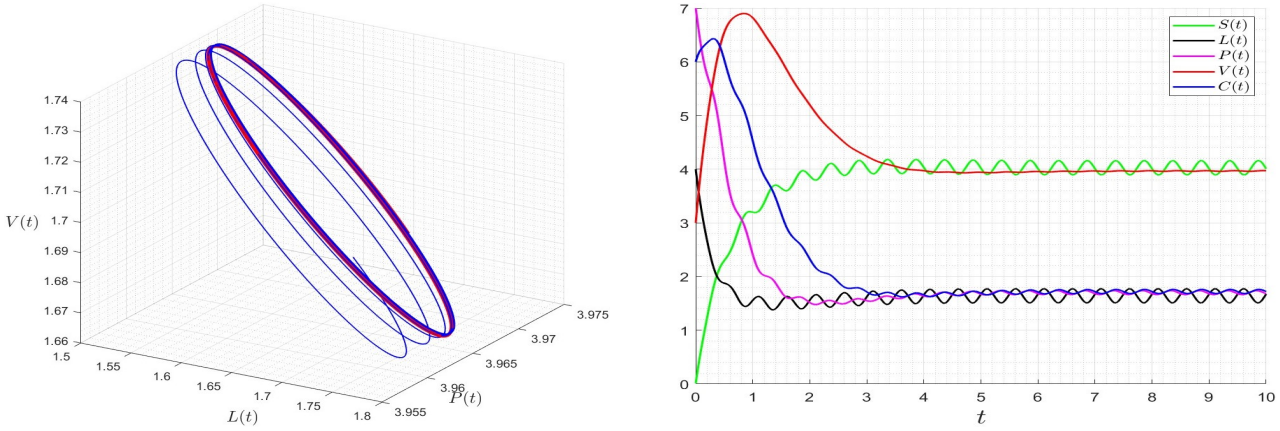

Figure 5. Dynamics of (3.3) for $\varphi_1^{max} = 0.2$, $\varphi_2^{max} = 0.3$, $\varphi_3^{max} = 0.4$, $k_1 = 1$, $k_2 = 2$, and $k_3 = 3$, with $\mathcal{R}_0 \approx 7.15 > 1$.

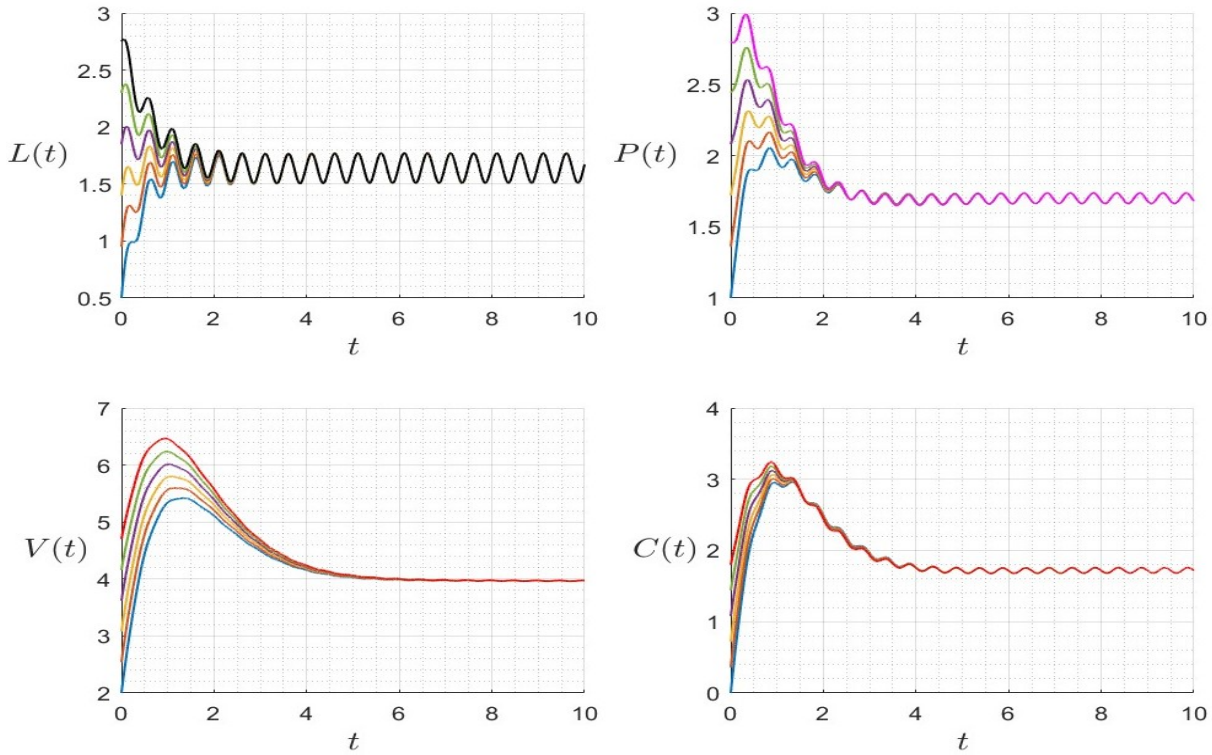

Figure 6. Behavior of the trajectories of (3.3) for several initial conditions when $\varphi_1^{max} = 0.2$, $\varphi_2^{max} = 0.3$, $\varphi_3^{max} = 0.4$, $k_1 = 1$, $k_2 = 2$, and $k_3 = 3$ ($\mathcal{R}_0 \approx 7.15 > 1$).

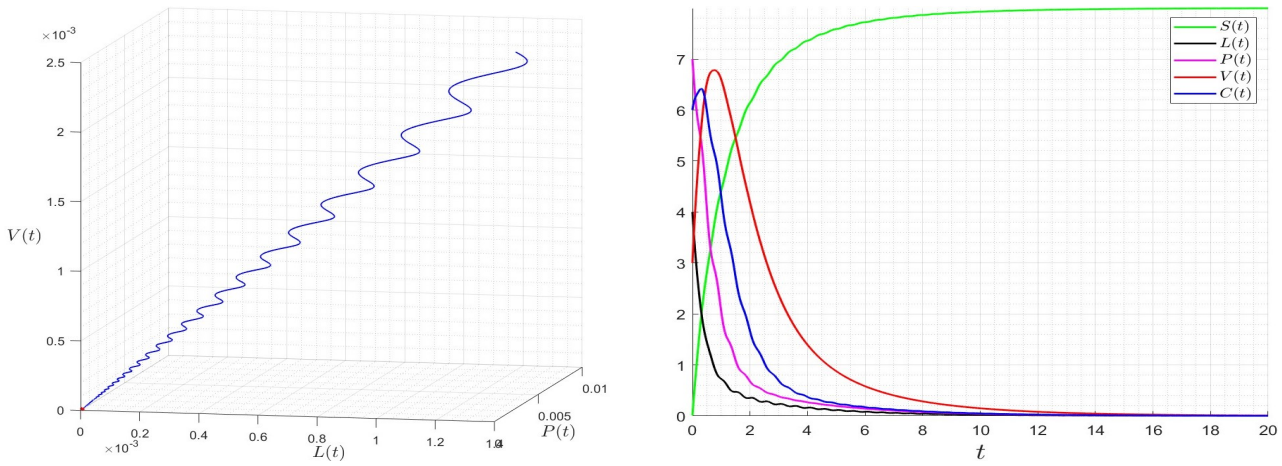

Figure 7. Dynamics of (3.3) for $\varphi_1^{max} = 0.1$, $\varphi_2^{max} = 0.2$, $\varphi_3^{max} = 0.3$, $k_1 = 12$, $k_2 = 12$, and $k_3 = 12$, with $\mathcal{R}_0 \approx 0.58 < 1$.

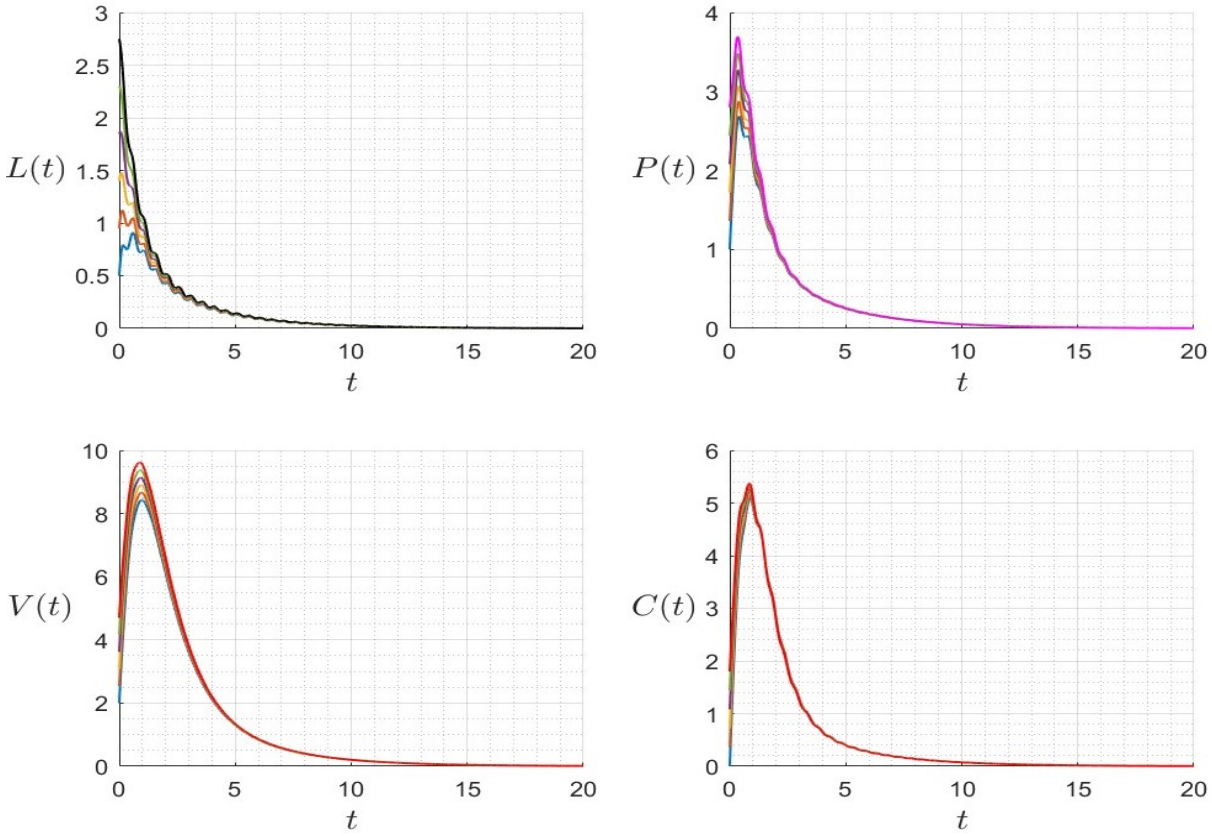

Figure 8. Behavior of the trajectories of (3.3) for several initial conditions when $\varphi_1^{max} = 0.1$, $\varphi_2^{max} = 0.2$, $\varphi_3^{max} = 0.3$, $k_1 = 12$, $k_2 = 12$, and $k_3 = 12$ ($\mathcal{R}_0 \approx 0.58 < 1$).

3.3. *Totally periodic environment*

In the third step, we assume that all parameters are ω-periodic functions, and the system is expressed as

$$\begin{cases} \dot{S}(t) = d_s(t)\Lambda(t) - d_s(t)S(t) - [\sigma_1(t)\varphi_1(V(t)) + \sigma_2(t)\varphi_2(L(t)) + \sigma_3(t)\varphi_3(P(t))]S(t), \\ \dot{L}(t) = [\sigma_1(t)\varphi_1(V(t)) + \sigma_2(t)\varphi_2(L(t)) + \sigma_3(t)\varphi_3(P(t))]f(S(t)) - (\eta_1(t) + d_l(t))L(t), \\ \dot{P}(t) = \eta_1(t)L(t) - d_p(t)P(t) - \sigma_4(t)\varphi_4(P(t))C(t), \\ \dot{V}(t) = \eta_2(t)P(t) - d_v(t)V(t), \\ \dot{C}(t) = \eta_3(t)P(t) - d_c(t)C(t) - \sigma_5(t)\varphi_5(P(t))C(t), \end{cases} \tag{3.4}$$

given an initial condition with non-negative values

$$(S^0, L^0, P^0, V^0, C^0) = (0.01, 4, 7, 3, 6) \in \mathbb{R}^5_+.$$

Again, as in the case of model (3.3), the time-averaged system was used to calculate $\mathcal{R}_0$. The behavior of the trajectories of (3.4) with respect to time is shown in Figure 9 (right), and in *LPV* coordinates in Figure 9 (left), where $\mathcal{R}_0 > 1$. As can be seen, the solution converges to a periodic trajectory, confirming *HIV* persistence. Several initial conditions were considered in Figure 10, and all trajectories converge to the same periodic trajectory. In Figure 11, we display the behavior of the trajectories of (3.4) in *LPV* coordinates (left) and the behavior of the trajectories with respect to time (right) for $\mathcal{R}_0 < 1$. Again, the theoretical results are confirmed, as the solution converges to the *HIV* disease-free periodic solution $\mathcal{A}_0(t) = (\Lambda^*(t), 0, 0, 0, 0)$, confirming *HIV* extinction. Several initial conditions were considered in Figure 12, and all trajectories converge to the same disease-free steady state.

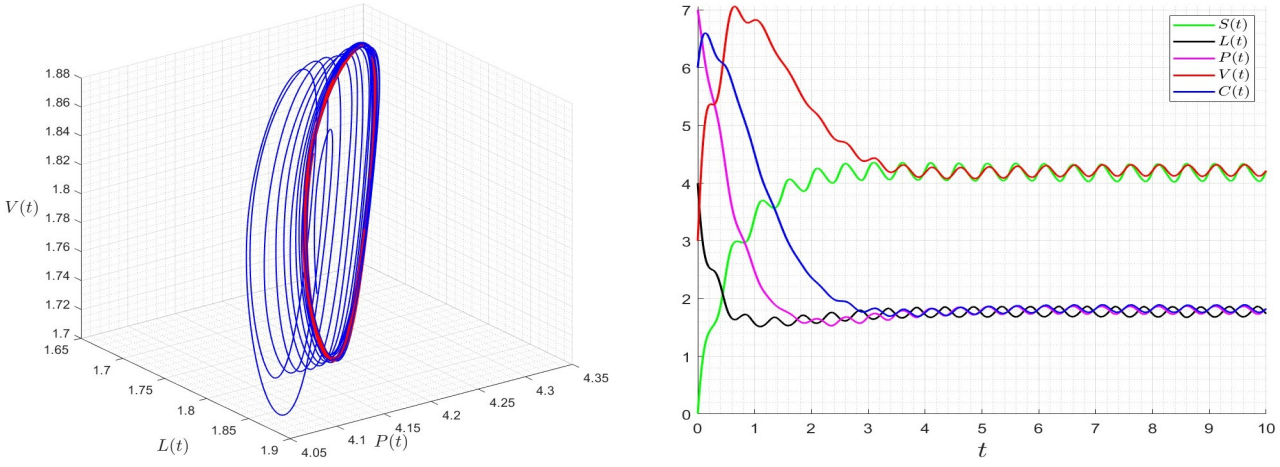

Figure 9. Dynamics of (3.4) for $\varphi_1^{max} = 0.2$, $\varphi_2^{max} = 0.3$, $\varphi_3^{max} = 0.4$, $k_1 = 1$, $k_2 = 2$, and $k_3 = 3$ ($\mathcal{R}_0 \approx 7.15 > 1$).

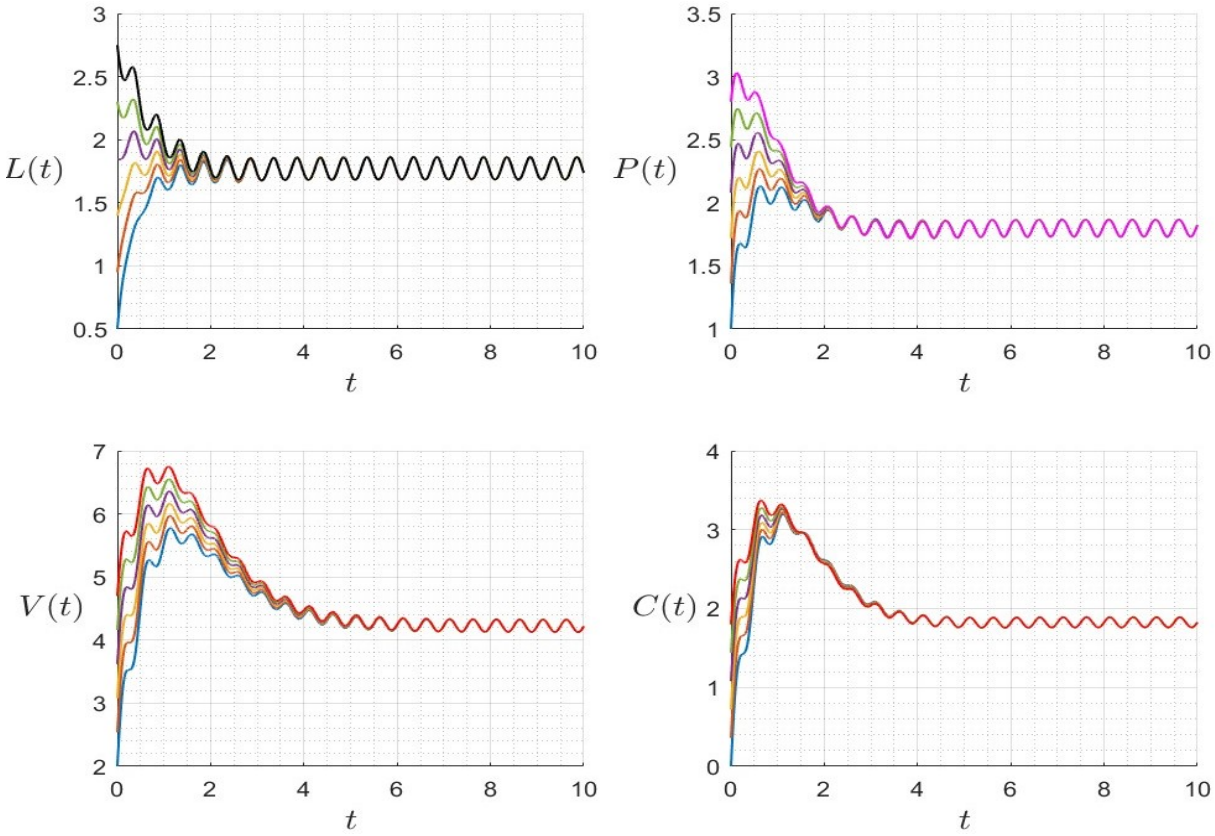

Figure 10. Dynamics of (3.4) for several initial conditions where $\varphi_1^{max} = 0.2$, $\varphi_2^{max} = 0.3$, $\varphi_3^{max} = 0.4$, $k_1 = 1$, $k_2 = 2$, and $k_3 = 3$ ($\mathcal{R}_0 \approx 7.15 > 1$).

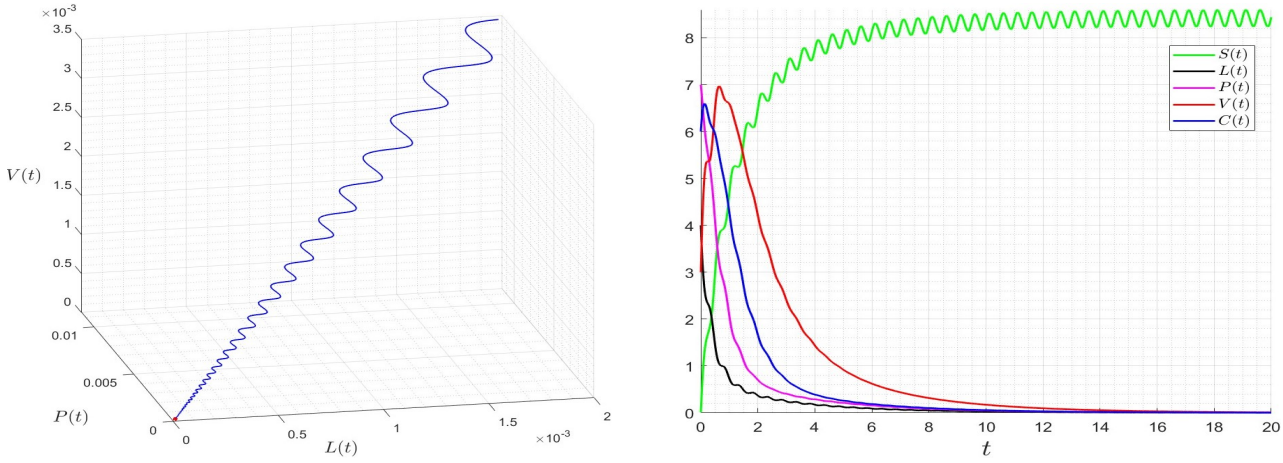

Figure 11. Dynamics of (3.4) for $\varphi_1^{max} = 0.1$, $\varphi_2^{max} = 0.2$, $\varphi_3^{max} = 0.3$, $k_1 = 12$, $k_2 = 12$, and $k_3 = 12$, with $\mathcal{R}_0 \approx 0.58 < 1$.

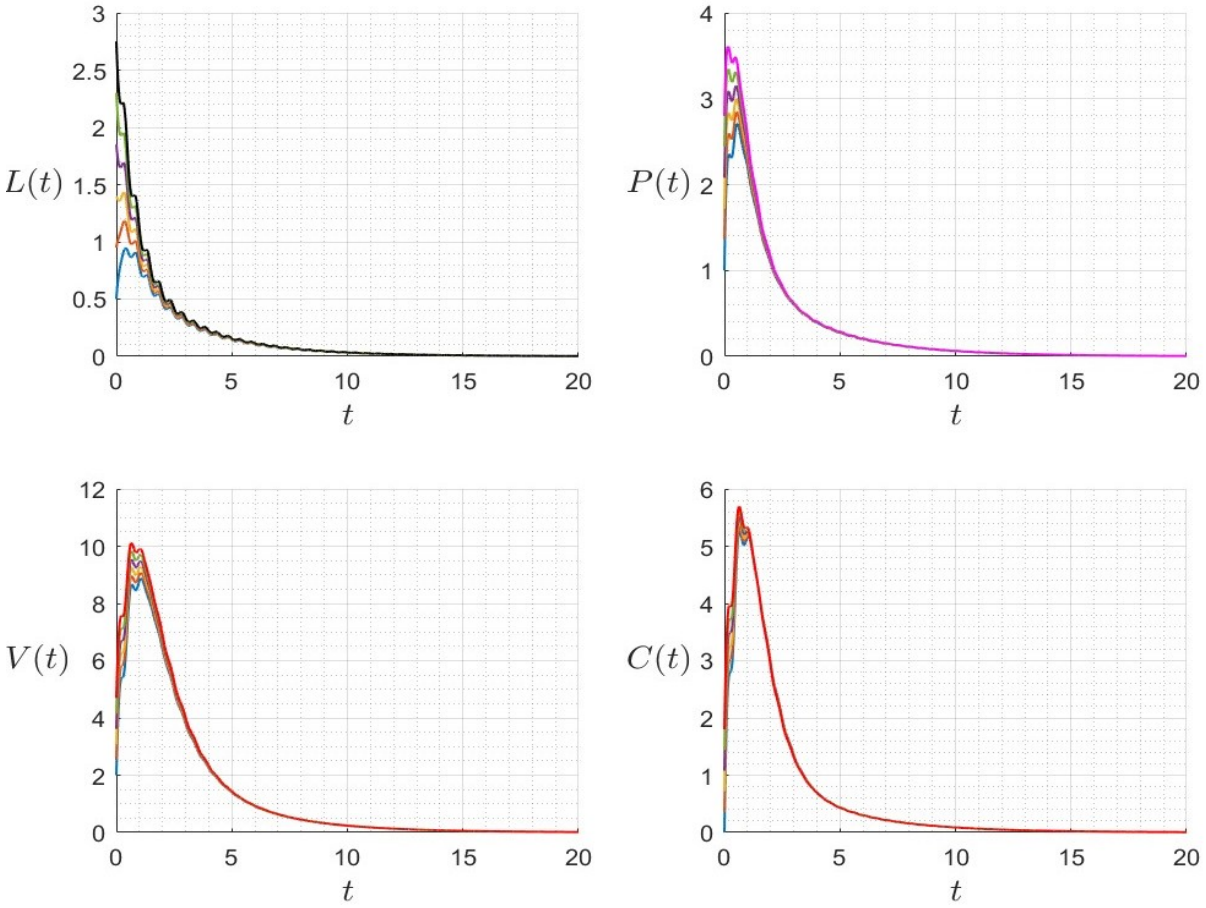

Figure 12. Dynamics of (3.4) for several initial conditions where $\varphi_1^{max} = 0.1$, $\varphi_2^{max} = 0.2$, $\varphi_3^{max} = 0.3$, $k_1 = 12$, $k_2 = 12$, and $k_3 = 12$ ($\mathcal{R}_0 \approx 0.58 < 1$).

4. Conclusions

This paper extends the system studied in [17], which models *HIV* transmission in blood cells by generalizing the infection, neutralization, and impairment rates. We defined the basic reproduction number $\mathcal{R}_0$ as the spectral radius of an integral operator. It is demonstrated that the *HIV*-free periodic solution $\mathcal{A}_0(t)$ is globally asymptotically stable when $\mathcal{R}_0 < 1$, and that *HIV* persists when $\mathcal{R}_0 > 1$, exhibiting asymptotic periodic behavior. We provide several numerical tests for three situations, fixed parameters, periodic transmission rates, and a fully periodic environment, all of which confirm the theoretical results, showing that the solution converges to a limit cycle.

Acknowledgments

The author is grateful to the anonymous reviewers for their valuable and constructive feedback, which helped improve the presentation of the paper.

Conflict of interest

The author declares no conflict of interest.

References

1. Q. Liu, D. Jiang, Dynamical behavior of a higher order stochastically perturbed HIV/AIDS model with differential infectivity and amelioration, *Chaos Soliton. Fract.*, **141** (2020), 110333. https://doi.org/10.1016/j.chaos.2020.110333
2. P. A. Naik, K. M. Owolabi, M. Yavuz, J. Zu, Chaotic dynamics of a fractional order HIV-1 model involving AIDS-related cancer cells, *Chaos Soliton. Fract.*, **140** (2020), 110272. https://doi.org/10.1016/j.chaos.2020.110272
3. M. Di Mascio, R. M. Ribeiro, M. Markowitz, D. D. Ho, A. S. Perelson, Modeling the long-term control of viremia in HIV-1 infected patients treated with antiretroviral therapy, *Math. Biosci.*, **188** (2004), 47–62. https://doi.org/10.1016/j.mbs.2003.08.003
4. S. Kumar, R. Kumar, J. Singh, K. S. Nisar, D. Kumar, An efficient numerical scheme for fractional model of HIV-1 infection of $CD4^+$ T-cells with the effect of antiviral drug therapy, *Alexandria Eng. J.*, **59** (2020), 2053–2064. https://doi.org/10.1016/j.aej.2019.12.046
5. R. Ullah, R. Ellahi, S. M. Sait, S. T. Mohyud-Din, On the fractional-order model of HIV-1 infection of $CD4^+$ T-cells under the influence of antiviral drug treatment, *J. Taibah Univ. Sci.*, **14** (2020), 50–59. https://doi.org/10.1080/16583655.2019.1700676
6. M. H. Alharbi, Global investigation for an "SIS" model for COVID-19 epidemic with asymptomatic infection, *Math. Biosci. Eng.*, **20** (2023), 5298–5315. https://doi.org/10.3934/mbe.2023245
7. F. K. Alalhareth, M. H. Alharbi, M. A. Ibrahim, Modeling typhoid fever dynamics: stability analysis and periodic solutions in epidemic model with partial susceptibility, *Mathematics*, **11** (2023), 3713. https://doi.org/10.3390/math11173713
8. M. H. Alharbi, F. K. Alalhareth, M. A. Ibrahim, Analyzing the dynamics of a periodic typhoid fever transmission model with imperfect vaccination, *Mathematics*, **11** (2023), 3298. https://doi.org/10.3390/math11153298
9. M. A. Ibrahim, A. Dénes, Stability and threshold dynamics in a seasonal mathematical model for measles outbreaks with double-dose vaccination, *Mathematics*, **11** (2023), 1791. https://doi.org/10.3390/math11081791
10. M. El Hajji, Periodic solutions for chikungunya virus dynamics in a seasonal environment with a general incidence rate, *AIMS Math.*, **8** (2023), 24888–24913. https://doi.org/10.3934/math.202312699
11. M. El Hajji, M. F. S. Aloufi, M. H. Alharbi, Influence of seasonality on Zika virus transmission, *AIMS Math.*, **9** (2024), 19361–19384. https://doi.org/10.3934/math.2024943
12. H. H. Almuashi, Mathematical analysis for the influence of seasonality on chikungunya virus dynamics, *Int. J. Anal. Appl.*, **22** (2024), 86. https://doi.org/10.28924/2291-8639-22-2024-86

13. F. A. Al Najim, Mathematical analysis for a Zika virus dynamics in a seasonal environment, *Int. J. Anal. Appl.*, **22** (2024), 71. https://doi.org/10.28924/2291-8639-22-2024-71

14. M. El Hajji, N. S. Alharbi, M. H. Alharbi, Mathematical modeling for a CHIKV transmission under the influence of periodic environment, *Int. J. Anal. Appl.*, **22** (2024), 6. https://doi.org/10.28924/2291-8639-22-2024-6

15. X. Wang, X. Song, Global stability and periodic solution of a model for HIV infection of $CD4^+$ T cells, *Appl. Math. Comput.*, **189** (2007), 1331–1340. https://doi.org/10.1016/j.amc.2006.12.044

16. M. El Hajji, R. M. Alnjrani, Periodic trajectories for HIV dynamics in a seasonal environment with a general incidence rate, *Int. J. Anal. Appl.*, **21** (2023), 96. https://doi.org/10.28924/2291-8639-21-2023-96

17. M. El Hajji, R. M. Alnjrani, Periodic behaviour of HIV dynamics with three infection routes, *Mathematics*, **12** (2024), 123. https://doi.org/10.3390/math12010123

18. V. G. Frobenius, Über matrizen aus nicht negativen elementen, *Sitzung Phys.-Math.*, **23** (1912), 456–477.

19. F. Zhang, X. Q. Zhao, A periodic epidemic model in a patchy environment, *J. Math. Anal. Appl.*, **325** (2007), 496–516. https://doi.org/10.1016/j.jmaa.2006.01.085

20. W. Wang, X. Q. Zhao, Threshold dynamics for compartmental epidemic models in periodic environmentss, *J. Dyn. Differ. Equat.*, **20** (2008), 699–717. https://doi.org/10.1007/s10884-008-9111-8

21. X. Q. Zhao, *Dynamical systems in population biology*, 1 Ed., New York: Springer-Verlag, 2003. https://doi.org/10.1007/978-0-387-21761-1

22. O. Diekmann, J. A. P. Heesterbeek, J. A. J. Metz, On the definition and the computation of the basic reproduction ratio $\mathcal{R}_0$ in models for infectious diseases in heterogeneous populations, *J. Math. Bio.*, **28** (1990), 365–382. https://doi.org/10.1007/BF00178324

23. P. Van den Driessche, J. Watmough, Reproduction numbers and sub-threshold endemic equilibria for compartmental models of disease transmission, *Math. Biosci.*, **180** (2002), 29–48. https://doi.org/10.1016/S0025-5564(02)00108-6

AIMS Press